

1987

Long-lifetime, reliable liquid metal ion sources for boron, arsenic, and phosphorus

W. M. Clark Jr.

R. L. Seliger

Mark Utlaut

University of Portland, utlaut@up.edu

A. E. Bell

L. W. Swanson

See next page for additional authors

Follow this and additional works at: http://pilotscholars.up.edu/phy_facpubs



Part of the [Plasma and Beam Physics Commons](#)

Citation: Pilot Scholars Version (Modified MLA Style)

Clark, W. M. Jr.; Seliger, R. L.; Utlaut, Mark; Bell, A. E.; Swanson, L. W.; Schwind, G. A.; and Jergenson, J. B., "Long-lifetime, reliable liquid metal ion sources for boron, arsenic, and phosphorus" (1987). *Physics Faculty Publications and Presentations*. 36.
http://pilotscholars.up.edu/phy_facpubs/36

This Journal Article is brought to you for free and open access by the Physics at Pilot Scholars. It has been accepted for inclusion in Physics Faculty Publications and Presentations by an authorized administrator of Pilot Scholars. For more information, please contact library@up.edu.

Authors

W. M. Clark Jr., R. L. Seliger, Mark Utlaut, A. E. Bell, L. W. Swanson, G. A. Schwind, and J. B. Jergenson

Long-lifetime, reliable liquid metal ion sources for boron, arsenic, and phosphorus

W. M. Clark, Jr., R. L. Seliger, and M. W. Utlaut
Hughes Research Laboratories, Malibu, California 90265

A. E. Bell, L. W. Swanson, and G. A. Schwind
Oregon Graduate Center, Beaverton, Oregon 97006

J. B. Jergenson
Jergenson Design and Manufacturing, Santa Barbara, California 93101

(Received 27 May 1986; accepted 13 October 1986)

Operation of liquid-metal ion sources based on palladium alloys that contain boron, arsenic, and phosphorus (singly or in combination) was studied. These sources, when run on refractory metal needles and heater ribbons, have exhibited high angular intensity ($1.5\text{--}5\ \mu\text{A}/\text{sr}$), long lifetime ($> 150\ \text{h}$), low energy spread ($< 15\ \text{eV}$), and stable operation with extracted currents down to $2\ \mu\text{A}$.

I. INTRODUCTION

Focused beams of ions have shown considerable promise for maskless processing of semiconductor devices in research performed at various facilities worldwide. Particular advantages of focused ion beam (FIB) processing of devices include:

(i) maskless implantation, which makes possible laterally varied implant doses of device-active areas that improve performance such as decreasing the Kirk effect caused by emitter current crowding in bipolar transistors¹;

(ii) metal layer patterning to provide FET gate contacts with a width of $0.1\ \mu\text{m}$ (Ref. 2);

(iii) high-resolution micromachining of grooves in semiconductor device thin films or integrated optical structures with a width down to $0.06\ \mu\text{m}$.³ Unfortunately, full utilization of this technology for silicon devices has been impeded, heretofore, by the absence of long-lifetime reliable sources that produce the primary dopant ion species (i.e., boron, arsenic, and phosphorus). Focused beams of boron have also been used to produce isolation regions in GaAs devices.⁴ Practical use of FIBs for device processing requires that the focused target current be large enough so that device throughput is good, i.e., the beam time to perform the required fabrication steps is appropriately small. This requires a minimum value of the ion source brightness, on the order of $\sim 10^6\ \text{A}/\text{cm}^2\ \text{sr}$. Previous work has shown that single-component liquid metal ion sources (LMIS) provide such a brightness.⁵

II. EXPERIMENTAL RESULTS

Liquid metal ion sources of Ga, In, Au, etc. were first demonstrated; however, elemental sources of the dopant species (e.g., B and As) are not possible because either the melting point or the vapor pressure is too high to be practical for use in an ion-focusing column. Use of liquid metal alloys, where the element of choice is alloyed with an appropriate carrier metal, demonstrated that focused beams of B and As could be produced from a LMIS using alloys such as $\text{Pt}_{0.72}\text{B}_{0.28}$, $\text{Pd}_{0.4}\text{Ni}_{0.4}\text{B}_{0.2}$, and $\text{Pd}_{0.4}\text{Ni}_{0.4}\text{As}_{0.1}\text{B}_{0.1}$ in an ion-focusing column with a Wien mass filter to separate the

ion species.⁶ Use of alloys has two advantages—the melting point of the alloy can be less than that of a single constituent, and volatile elements such as arsenic may be chemically bound sufficiently for operation in a vacuum enclosure. Practical operation of the alloys mentioned above for dopant ion sources has proved unsatisfactory because of chemical corrosion reactions that occur between the liquid metal and the needle and heater ribbon substrate.

We report the operation of liquid-metal ion sources for boron, arsenic, and phosphorus, which run on the simple source structure shown in Fig. 1, and possess the desirable characteristics of brightness, stability, and long life.

A. Arsenic

The typical *n*-type dopant elements for silicon devices are arsenic, phosphorus, and antimony; each of these has too large a vapor pressure at its melting point to be used as an elemental LMIS in a vacuum system. Hence, an alloy LMIS for these ions must decrease the effective vapor pressure by providing either a very low melting temperature, or by chemically tying up the volatile elements. We have performed experiments with the alloy systems PbAuAs and PbAuSb, which have very low melting points ($< 200\ ^\circ\text{C}$). We were able to obtain operational LMIS with these, but found that the range of temperatures over which the alloy would not release As or Sb was very small ($< 50\ ^\circ\text{C}$ above melting). This is not practical for a LMIS using the heater ribbon structure shown in Fig. 1 because there are regions on the

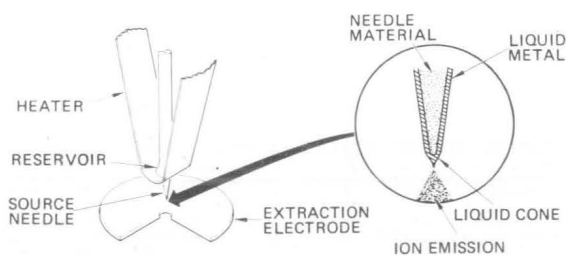
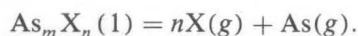


FIG. 1. Liquid metal ion source (LMIS) structure.

ribbon having temperatures more than 50 °C higher than at the needle tip. Hence, alloy material wetting the heater ribbon in these areas would vaporize.

Selecting a binary system that could have the desired low vapor pressure for arsenic at the melting point may be approached by considering the Gibbs free energy of formation for compounds of the binary constituents. For example, for a given arsenic compound such as $As_m X_n$, where X is a low volatility element, the equilibrium condition between vapor and liquid is



The equilibrium constant for this reaction is

$$K(p) = P^n(As)P^m(X),$$

and the Gibbs free energy is

$$\Delta G = -RT \ln K(p).$$

Hence, if ΔG has a large negative value, then $K(p)$ and $P(As)$ will be smaller, typically, than in the case of an ideal solution (no compound formation) of the same elemental constituents. This is because nonideal (compound) solutions are more stable than ideal solutions because of the existence of chemical-bonding forces between the chemical species. Examination of the binary phase diagram of the Pd-As alloy⁷ systems shows the presence of several compounds. This suggests that the Pd-As chemical bonding might be large enough to reduce the chemical activity of arsenic in a LMIS. In addition, SOLGASMIX calculations for the equilibrium vapor pressures at the melting points of various Pd-As species indicated that the compound Pd_2As would be congruently vaporizing.⁸ Therefore, a LMIS was made with Pd_2As utilizing a tungsten needle and heater ribbon assembly. The Pd_2As material is observed to melt at a temperature of 1035 ± 5 K (measured with an optical pyrometer through a Pyrex vacuum-viewing window), but does not wet and flow over the tungsten until the temperature is raised another 100–200 °C. After wetting, the temperature may be reduced almost to the melting point for source operation. We operated the source at much higher temperatures, up to 1400 K, with no indication of loss of arsenic. A mass spectrum of the source, taken in a three-lens, mass-separating, ion-focusing column⁶ is shown in Fig. 2. From the mass spectrum, it is noted that:

(i) both singly and doubly ionized species of arsenic are available in sufficient amounts;

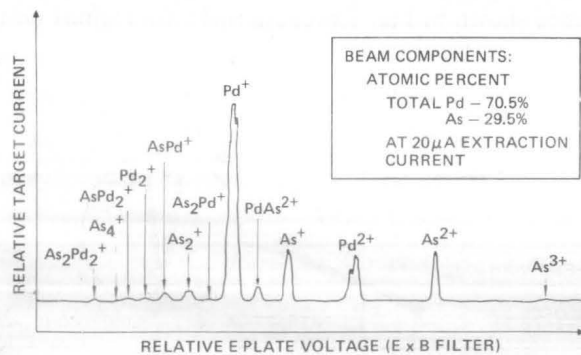


FIG. 2. Mass spectrum of a liquid-metal ion source using Pd_2As on a tungsten substrate.

(ii) the total amount of emitted Pd and As is in nearly the stoichiometric ratio of the compound (i.e., 2:1 Pd:As).

Precise determinations of the mass spectrum and energy spreads for the emitted species were obtained with a Hitachi RMU-7 magnetic sector mass spectrometer with a CuBe discrete dynode detector. Pressure in the source chamber was 1×10^{-7} Torr and the emitter temperature was measured by a micropyrometer. The entrance slit to the mass spectrometer subtended a 2 mrad angle at the emitter. Relative amounts of the mass species as a function of total extraction current were determined by measuring the area under the respective peaks. No correction was made for the variation of the mass dependence of the spectrometer sensitivity. Total energy distributions were determined by measuring the full width at half-maximum (FWHM) of mass spectrometer peaks. The intrinsic FWHM of the assumed Gaussian transmission window of the mass spectrometer was measured to be 4.3 eV and was subtracted in quadrature from the measured values of the FWHM. The experimentally observed functional dependence of FWHM of the energy spread for the principal species from the Pd_2As source is shown in Fig. 3, plotted vs the total extraction current, and taken at a temperature of 1125 K. One can conclude from these data that the energy spread ΔV increases with extraction current I and mass m , and decreases with the charge (which agrees with most theoretical models).⁹

The source angular intensity was measured using two different ion-focusing systems. With the three-lens system, at a total extraction current of $20 \mu A$, the doubly ionized arsenic current at the target was 30 pA, with a beam acceptance half-

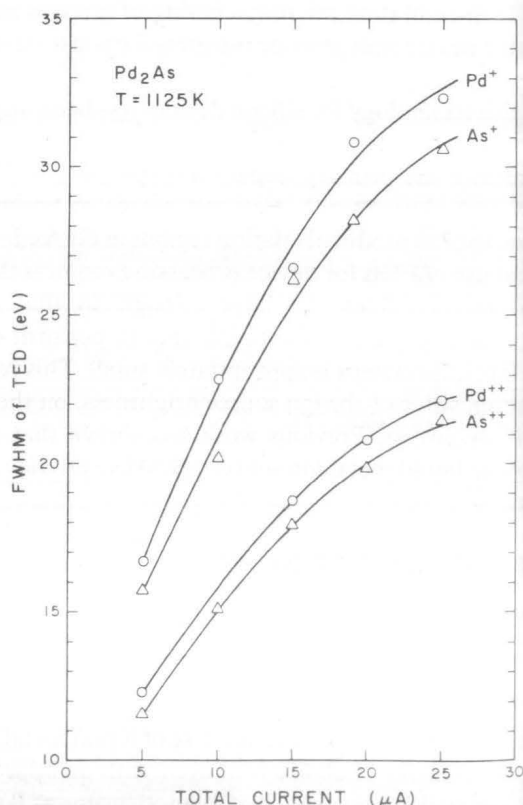


FIG. 3. Energy spread measured as the full width at half-maximum (FWHM) of the total energy distribution for the indicated principal beam species as a function of source current for the Pd_2As LMIS.

angle of 1.5 mrad. From this, the arsenic source angular intensity for the doubly ionized species is calculated as $5 \mu\text{A}/\text{sr}$. More extensive data were taken utilizing a simpler system, with no lenses, in which the beam is defined by the source needle and a beam-defining aperture located downstream of the extraction electrode (to give a beam half-angle of 1 mrad) and the current collected in a Faraday cup. Angular intensity values for individual components in the beam are then calculated using the beam fractions determined by the mass analyzer (as described above). With this system, the variation of source angular intensity plotted vs extractor current is shown in Fig. 4. Here it is seen that the angular intensity for As^{++} is comparable to the values obtained with the three-lens system and is larger than As^+ throughout the range measured.

The behavior of these sources during operation in the three-lens focusing column is excellent. Positional and electrical stability is good enough that a source can run an entire day with almost no adjustment of the column focus controls. Such stable performance is maintained to extraction currents as low as $2 \mu\text{A}$. Figure 5 shows typical I-V characteristics for sources with two different Pd alloys containing arsenic. The slope of the I-V characteristic for a source using Pd_2As is $120 \text{ nA}/\text{V}$, which compares with $\sim 20 \text{ nA}/\text{V}$ reported for elemental sources of gold¹⁰ and gallium,⁵ and alloy sources with $\text{Au}_{0.82}\text{Si}_{0.18}$ and $\text{Pt}_{0.72}\text{B}_{0.28}$. Hence, the slope of this Pd-As source is steeper than that obtained with other sources and indicates that the flow of liquid alloy from the reservoir down to the needle tip supplies the required alloy material as the voltage is raised (without severe limitations resulting from surface tension, viscosity, or corrosion-

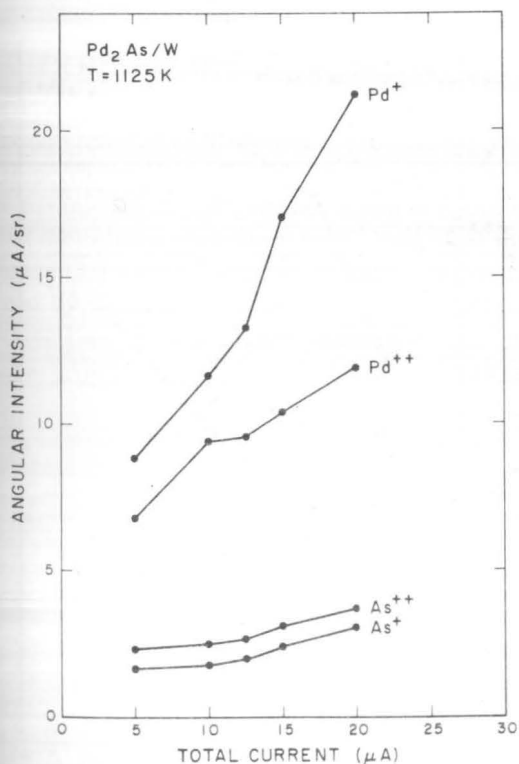


FIG. 4. Angular intensity of the emitted current for the indicated principal beam species for the Pd_2As LMIS as a function of the total extracted current.

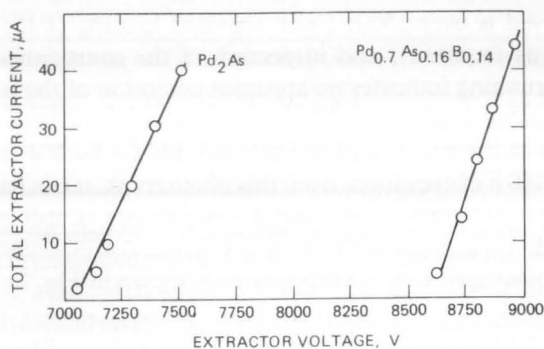


FIG. 5. Dc I-V characteristics for ion sources with Pd_2As and $\text{Pd}_{0.7}\text{As}_{0.16}\text{B}_{0.14}$ liquid metals.

induced effects). Source lifetime exceeds 150 h, with repeated loading of new alloy material when necessary. In our implantation experiments, all the sources tested operated over 50 h, with the termination occurring when the source ran out of fuel. Inspection of the source modules after running out of fuel does not indicate that any corrosive reaction between the liquid alloy and the tungsten needle and heater ribbon has taken place. A sample of the alloy was placed on a flat strip of tungsten heater ribbon and current was passed to melt the alloy. After 150 h of operation at 50°C above the melting point, there was still no indication of corrosion of the tungsten ribbon or any evidence, via Auger spectroscopy, of tungsten on the alloy surface.

B. Boron and arsenic

Obtaining both boron and arsenic from a single liquid-metal ion source means that both *n*- and *p*-type active regions can be implanted in device structures requiring them (such as bipolar devices and CMOS circuits), without having to break the system vacuum and change sources. Previous experiments run with $\text{Pd}_{0.4}\text{Ni}_{0.4}\text{B}_{0.1}\text{As}_{0.1}$ obtained a beam of arsenic ions, but essentially no boron.⁶ This failure to obtain boron was attributed to:

(i) possible migration of the boron into the needle and heater ribbon material (carbonized tungsten);

(ii) the fact that the difference between field evaporation thresholds for B (the highest) and Ni (the lowest) is larger than for the other alloy constituents. (The required electrical field for field evaporation of pure boron is $6.5 \text{ V}/\text{A}$; for Pd, $3.8 \text{ V}/\text{A}$; for Ni, $3.4 \text{ V}/\text{A}$; and for As, $4.55 \text{ V}/\text{A}$.)¹¹

Using an alloy with an approximate composition of $\text{Pd}_{0.7}\text{As}_{0.16}\text{B}_{0.14}$, we have produced a source with adequate brightness for both boron and arsenic. This alloy has been made in two ways:

(i) by mixing equal amounts of Pd_2As and Pd-B eutectic (72:28 atomic ratio) in a quartz holder and heating until the mixture melts, and (ii) by combustion synthesis of a mixture of all three components. Best source operation was obtained using a source configuration consisting of a tungsten needle and a rhenium heater ribbon. This source has the same stability characteristics, even at low extraction currents, as the Pd_2As source. The slope of the I-V characteristic shown in Fig. 5 is $\sim 100 \text{ nA}/\text{V}$, which is also higher than that obtained with other LMISs. The maximum source lifetime we have

observed is over 150 h (with repeated loading of the new alloy as required), and inspection of the source modules after running indicates no apparent corrosion of the needle and heater ribbon materials. Figure 6 shows an SEM photograph of the needle and ribbon assembly for such a source after 150 h of operation; from this photograph, it can be seen that the integrity of the metal components is still maintained.

A mass spectrum for this source is shown in Fig. 7. Note that the boron fraction in the beam is less than that in the alloy; this is possibly an indication of the effects of the relatively large evaporation-field threshold for boron. Nevertheless, the amount of boron obtained is sufficient for practical use in the focusing column. Angular intensity measurements were taken with the same instrument as that described above and are shown in Fig. 8. Here it is noted that the value of angular intensity $dI/d\Omega$ for As^{++} is substantially the same as that obtained with sources using Pd_2As . Hence, the presence of the boron in the alloy does not decrease arsenic ion emission (probably because of the lower evaporation field threshold for arsenic compared with boron). Figure 9 shows measurements of the energy spread of some of the emitted species (plotted vs the total extracted current).

C. Phosphorus

Phosphorus is an n -type dopant for Si devices; it is used in special applications such as threshold adjustment for FET devices and to set a deep well for subsequent base implants in vertical n - p - n bipolar devices. Accordingly, the doubly ionized species of phosphorus is desirable. We tried running a source using Pd_3P on a tungsten substrate assembly. This material melted above 1275 K, but the electrical performance was quite unstable. We then mixed equal parts of melted Pd_2As , Pd - B eutectic, and Pd_3P to form an alloy with the approximate composition of $Pd_{0.64}As_{0.11}B_{0.09}P_{0.16}$. With this alloy, we made a source that has produced the mass spectrum shown in Fig. 10. Usable amounts of As , B , and doubly and singly ionized P are obtained as shown. As with the other Pd -based alloy sources we have described, this source ran stably and, for the lengths of time we tested (25 h), no corrosion of the metal components was observed.

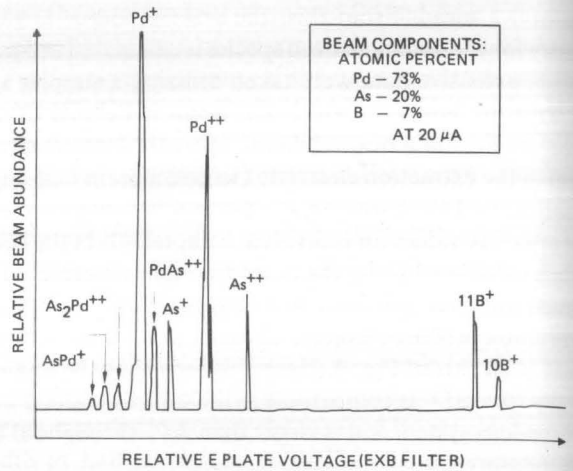


FIG. 7. Mass spectrum of the beam from a LMIS with $Pd_{0.70}As_{0.16}B_{0.14}$ alloy, a tungsten needle, and a rhenium heater ribbon.

III. DISCUSSION

The usefulness of the sources we describe (and any LMIS) depends on whether they produce the desired focused spot with sufficient target current. An estimate of source performance in this regard, as shown in the following discussion, may be determined by the ratio $I' / (\Delta V)^2$, where $I' = dI/d\Omega$ the angular intensity of the emitted current and ΔV is the energy spread of the emitted ions.

The energy broadening ΔV caused by the stochastic Coulomb interactions in a charged particle beam diverging from a point source has been determined both theoretically¹² and experimentally to be

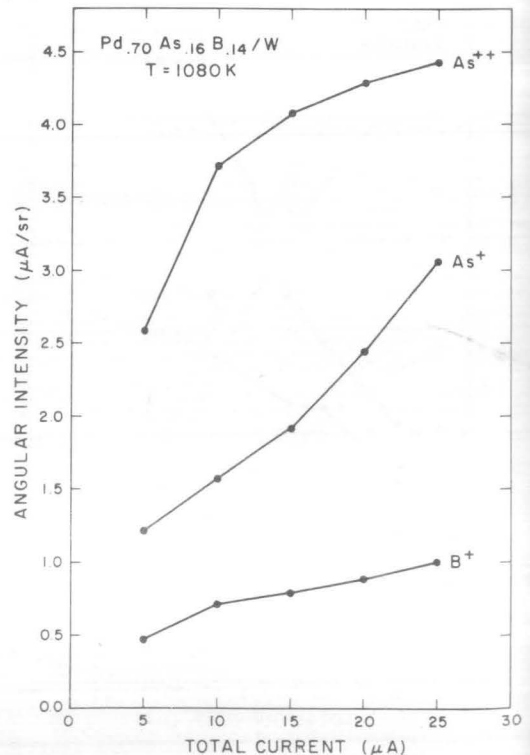


FIG. 8. Angular intensity of the emitted current of the principal beam species vs the total extracted current for a $PdAsB$ LMIS.

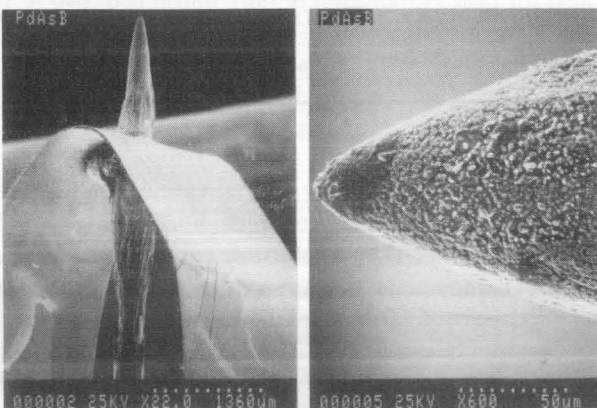


FIG. 6. Scanning electron micrographs of the tungsten needle and rhenium heater ribbon assembly of a $PdAsB$ LMIS after 150 h operation.

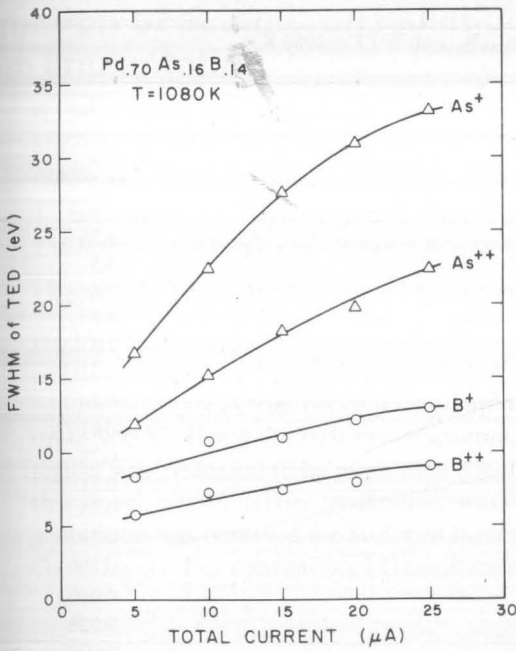


FIG. 9. Energy spread measured as the full width at half-maximum (FWHM) of the total energy distribution as a function of source current for principal species emitted from a PdAsB LMIS.

$$\Delta V_i^2 = \Delta V_0^2 + [K_1(I m_i^{1/2})^n]^2, \quad (1)$$

where n typically varies from 1/2 to 1, I is the total current, m_i is the mass of the i th species, and ΔV_0 is the intrinsic beam energy spread (i.e., at $I = 0$). For a focusing column limited by chromatic aberrations, which is usually the case with ions, one can derive the following relationship¹³ between the focused beam current density J_i and particle angular intensity I_i :

$$J_i = 4I_i'(V/\Delta V_i C_c M)^2, \quad (2)$$

where V , C_c , and M are the extraction voltage, chromatic aberration (referred to the source), and column magnification, respectively. From Eq. (2), we note that the ratio of source parameters $I_i'/\Delta V_i^2$ defines a source figure of merit and that the column parameters are C_c and M . It should be mentioned that source extraction voltage V is primarily determined by the source/extractor electrode geometry. By combining Eqs. (1) and (2) and noting that

$$I' = I_0 + K_2 I^m, \quad (3)$$

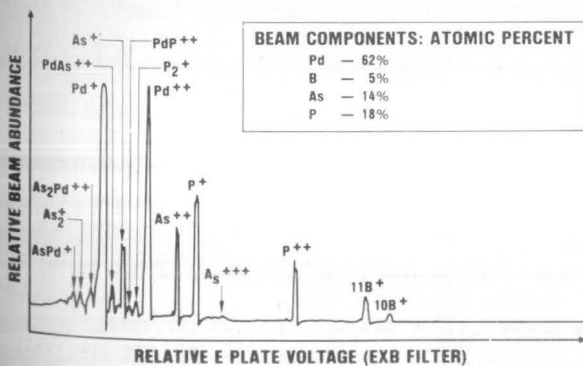


FIG. 10. LMIS tungsten needle wetted with Pd_{0.72}B_{0.28} eutectic alloy.

one can obtain

$$J_i = f(I, m, n). \quad (4)$$

For high currents, Eq. (4) becomes

$$J_i \sim 4(K_2/K_1^2)(I^{m-2n})/m^n, \quad (5)$$

and the value of J_i may increase or decrease with I , depending on the sign of $m - 2n$. For most single-component systems investigated so far, J_i is found to decrease with increasing I . Also, according to Eq. (5) and confirmed by experimental results, J_i always decreases for increasing mass of the i th particle. Of particular interest in this study is whether the conclusions implicit in Eq. (5) hold as well for a multicomponent LMIS.

Figures 3, 4, 8, and 9 show the experimental values of ΔV (full width at half-maximum) and I' vs I for both the Pd₂As and Pd_{0.7}As_{0.16}B_{0.14} alloy sources in the extractor current range from 5 to 25 μA. The ΔV vs I results for the Pd species in the ternary alloy were nearly identical to that of the binary alloy and, therefore, were not included in Fig. 9. For both alloy sources, the total angular intensity increased linearly with I ; thus, the nonlinearity seen, e.g., in the As⁺⁺ results in Fig. 8 is a result of a change in the relative abundance of all detected species for the Pd₂As and Pd_{0.7}As_{0.16}B_{0.14} LMISs obtained by comparing peak areas from the mass spectrometer results at the indicated source current.

From the results shown in Figs. 3, 4, 8, and 9, the variation of the source figure of merit with I can be obtained as shown in Fig. 11 for the species of interest. Here we see manifestation of the conclusion mentioned above for a single-component LMIS—no increase in the focused beam current den-

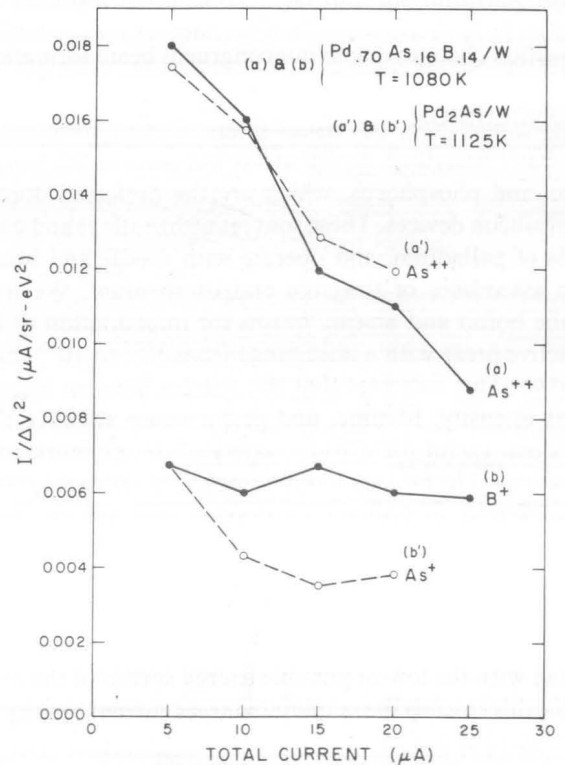


FIG. 11. The LMIS figure of merit, $I'/\Delta V^2$, as a function of source current for the indicated emitted species and alloy LMIS.

TABLE I. Percent abundance of various elements in beam at 20 μA for Pd_2As on W ($T = 1125\text{ K}$).

Elements	%
Pd^+	55.3
Pd^{++}	15.5
As^+	8.0
As^{++}	6.1
AsPd^{++}	5.5
AsPd^+	2.2
As_2^+	3.0
AsPd_2^{++}	1.3
As_2Pd^+	1.0
$\text{As}_3\text{Pd}^{++}$	0.85
AsPd_2^+	0.65
As_3^+	0.19
Pd^+	0.17
Pd_3^+	0.08
As^{+3}	0.03
Total Pd	70.5
Total As	29.5

sity can be achieved by increasing I in a chromatically limited column. In fact, for both alloy LMISs, J_{As} decreases with increasing I for both singly and doubly charged species. On the other hand, J_{B} for the ternary remains almost independent of I . Both sources exhibit an identical figure of merit for As^{2+} .

A favorable result noted in the summaries of Tables I and II is the congruency between the elemental stoichiometries in the bulk alloy and the beam. This is particularly true for the Pd_2As results. Congruent beam formation is most desirable for an alloy LMIS since source instability caused by variation in the melting point will occur as the bulk alloy composition changes due to noncongruent beam formation.

IV. CONCLUSION

We have described liquid-metal ion sources for boron, arsenic, and phosphorus, which are the preferred dopant ions for silicon devices. These sources utilize alloys and compounds of palladium, and operate with needle and heater ribbon assemblies of tungsten and/or rhenium. We have used the boron and arsenic beams for implantation of device-active areas with a dose range from 10^{12} to 10^{15} cm^{-2} (Ref. 14). This indicates that the sources have an angular current intensity, lifetime, and performance stability that make them useful for a wide variety of device fabrication applications. The PdAsB alloy source has the advantage that both preferred n - and p -type dopant ions are obtained; hence, both kinds of implants can be performed without breaking the ion-focusing column vacuum in order to change sources. Stable performance of these sources at low total extractor current enables the focusing column to be operated with the lowest possible energy spread of the emitted ions; this ensures the maximum target current density for a given small spot size.

The results described above indicate that the need has been fulfilled for sources that enable practical device fabrication utilizing focused beams of the dopant ions of boron,

TABLE II. Percent abundance of various elements in beam at 20 μA for $\text{Pd}_{0.70}\text{As}_{0.16}\text{B}_{0.14}$ on W ($T = 1080\text{ K}$).

Elements	%
Pd^+	53.3
Pd^{++}	15.7
As^{++}	5.8
As^+	6.7
AsPd^{++}	3.5
B^+	2.4
PdB^+	4.2
PdAs^+	1.8
As^{++}	1.6
$\text{Pd}_2\text{As}^+/\text{As}_3^+$	1.4
Pd_2As^+	0.91
PdAs_2	0.78
Pd_3	0.51
$\text{Pd}_2\text{As}^{++}$	0.45
Pd_2^+	0.23
PdAs_2^{++}	0.20
As^{+3}	0.040
PdB^{++}	0.026
B^{++}	0.0020
Total Pd	72.9
Total As	20.4
Total B	6.7

arsenic, and phosphorus. Further research on these sources is needed to find a boron source with a larger angular intensity, to optimize the alloy constituencies to provide larger beam fractions for various ion species, and to better understand the role of arsenic or other alloy constituents in preventing corrosion of metal source components by the liquid alloy. A more comprehensive understanding of the relation between relative abundance of various emitted ions on the evaporation field threshold and chemical activity between species is also desired. The apparent insensitivity to extraction current of the energy spread for emitted beams of boron also merits further study.

- ¹R. L. Reuss, D. Morgan, E. W. Greeneich, W. M. Clark, Jr., and D. B. Rensch, *J. Vac. Sci. Technol. B* **3**, 62 (1985).
- ²D. B. Rensch, J. Y. Chen, W. M. Clark, Jr., and M. D. Courtney, *J. Vac. Sci. Technol. B* **3**, 286 (1985).
- ³R. L. Seliger, R. L. Kubena, R. D. Olney, J. W. Ward, and V. Wang, *J. Vac. Sci. Technol.* **16**, 1610 (1979).
- ⁴H. Arimoto, A. Takamori, E. Miyauchi, and H. Hashimoto, *Jpn. J. Appl. Phys.* **23**, L165 (1984).
- ⁵L. W. Swanson, G. A. Schwind, and A. E. Bell, *J. Appl. Phys.* **51**, 3453 (1980).
- ⁶V. Wang, J. W. Ward, and R. L. Seliger, *J. Vac. Sci. Technol.* **19**, 1158 (1981).
- ⁷F. A. Shunk, *Constitution of Binary Alloys*, 2nd supplement (McGraw-Hill, New York, 1969), p. 59.
- ⁸R. P. Santandrea, Los Alamos National Laboratories (private communication).
- ⁹G. H. Jansen, T. R. Groves, and W. Stickel, *J. Vac. Sci. Technol. B* **3**, 190 (1985).
- ¹⁰A. Wagner and T. M. Hall, *J. Vac. Sci. Technol.* **16**, 1871 (1979).
- ¹¹D. G. Brandon, *Surf. Sci.* **3**, 1 (1964).
- ¹²M. A. Gesley and L. W. Swanson, *J. Phys.* **45**, 167 (1984).
- ¹³L. W. Swanson, *Nucl. Instrum. Method Phys. Res.* **218**, 347 (1983).
- ¹⁴R. H. Reuss, D. Morgan, A. Goldenetz, W. M. Clark, Jr., D. B. Rensch, M. W. Utlaut, *J. Vac. Sci. Technol. B* **4**, 290 (1986).